

Raman scattering studies of spin, charge, and lattice dynamics in $\text{Ca}_{2-x}\text{Sr}_x\text{RuO}_4$ ($0 \leq x < 0.2$)

H. Rho,^{1,2} S. L. Cooper,¹ S. Nakatsuji,³ H. Fukazawa,³ and Y. Maeno,^{3,4}

¹*Department of Physics and Frederick Seitz Materials Research Laboratory,
University of Illinois at Urbana-Champaign, Urbana, Illinois 61801*

²*Department of Physics, Chonbuk National University, Chonju 561-756, Korea*

³*Department of Physics, Kyoto University, Kyoto 606-8502, Japan*

⁴*International Innovation Center, Kyoto University, Kyoto 606-8501, Japan*

(Dated: November 12, 2018)

Abstract

We use Raman scattering to study spin, charge, and lattice dynamics in various phases of $\text{Ca}_{2-x}\text{Sr}_x\text{RuO}_4$. With increasing substitution of Ca by Sr in the range $0 \leq x < 0.2$, we observe (1) evidence for an increase of the electron-phonon interaction strength, (2) an increased temperature-dependence of the two-magnon energy and linewidth in the antiferromagnetic insulating phase, and (3) evidence for charge gap development, and hysteresis associated with the structural phase change, both of which are indicative of a first-order metal-insulator transition (T_{MI}) and a coexistence of metallic and insulating components for $T < T_{MI}$.

PACS numbers: 71.30.+h, 75.30.-m, 75.50.Ee, 78.30.-j

Single-layered ruthenates have drawn much experimental and theoretical attention due to both their structural similarity to the high- T_c cuprates, and their strongly correlated magnetic, electronic, phononic, and orbital degrees of freedom, which result in a rich phase diagram and exotic phenomena.^{1,2,3,4,5,6,7,8,9,10} $\text{Ca}_{2-x}\text{Sr}_x\text{RuO}_4$ (CSRO) exhibits various ground states with increasing substitution of Sr for Ca, ranging from antiferromagnetic (AF) insulating for $x = 0$ to superconducting for $x = 2$.^{1,2,3,4,5,6,7,8,9,10,11} For example, Sr_2RuO_4 ($T_c = 1.5$ K) is a spin-triplet superconductor which is isostructural to high- T_c cuprates such as $\text{La}_{2-x}\text{Ba}_x\text{CuO}_4$ ($T_c = 30$ K).¹ Unlike the doping driven high- T_c cuprates, however, the CSRO system is a bandwidth driven system: an increase of Ca content significantly distorts the RuO_6 -octahedra and decreases the 4d-band width, W , relative to the large effective Coulomb energy, U . As a result, the ground state for $x < 0.2$ is a Mott-like AF insulator.^{5,6,7,8} With increasing temperature, CSRO for $x < 0.2$ undergoes a metal-insulator (MI) transition. For instance, in Ca_2RuO_4 , AF ordering occurs below $T_N = 113$ K, and a MI transition occurs at $T_{MI} = 357$ K.^{9,10} Slight substitution of Ca by Sr ($0 < x < 0.2$) leads to a change of both T_N and T_{MI} . The MI transition is first-order and is accompanied by a simultaneous structural change with thermal hysteresis. In this Ca-rich region, Lee et al. have studied the temperature-dependent evolution of the optical conductivity, finding an important role of the electron-phonon interaction in governing the orbital arrangements, and suggesting a possible coexistence of antiferro-orbital and the ferro-orbital ordering states in the insulating phase.⁴ In addition, Nakatsuji et al. recently suggested that CSRO exhibits cooperative orbital ordering through the MI transition in the region $0 \leq x < 0.2$.⁸

All of these results suggest that there are very strong correlations among the spin, charge, lattice, and orbital degrees of freedom in CSRO for $x < 0.2$. In this Communication, we use the unique ability of Raman scattering to explore simultaneously magnetic, electronic, and structural dynamics, in order to investigate the interplay of the spin, charge, and lattice degrees of freedom in CSRO ($0 \leq x < 0.2$) through the AF ordering and MI transitions.

All single crystal samples, grown by a floating zone technique,^{5,9,11} were mounted inside a continuous He-flow cryostat. B_{1g} symmetry Raman spectra in the crossed polarization configuration were obtained using a Kr-ion laser with the 647.1 nm excitation wavelength in a backscattering geometry along the c -axis. Scattered light was dispersed through a triple spectrometer, and recorded using a liquid-nitrogen-cooled CCD detector. All the spectra were corrected, first, by removing the CCD dark current response, and then by normalizing

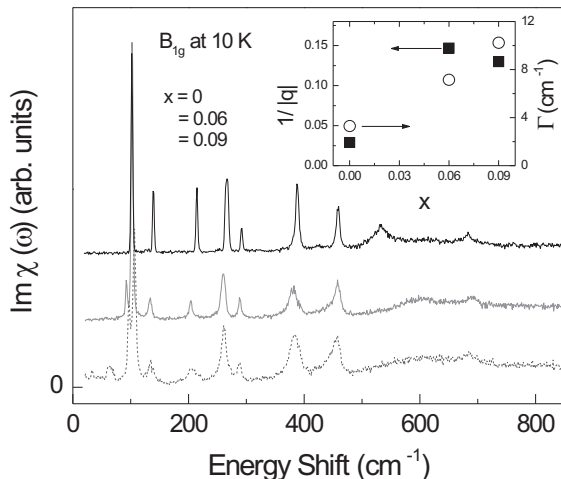


FIG. 1: Raman scattering spectra of CSRO for $x = 0, 0.06,$ and 0.09 from top to bottom, respectively. Spectra for $x > 0$ are shifted vertically for clarity. The inset shows the asymmetry parameter (filled squares) and linewidth (open circles) changes as a function of x for the 456 cm^{-1} B_{1g} phonon mode.

the spectrometer response using a calibrated white light source.

Figure 1 shows the $T = 10 \text{ K}$ Raman scattering spectra from CSRO for $x = 0, 0.06,$ and 0.09 . There are several key features and trends apparent in the spectra: (i) numerous phonon lines superimposed on the broad electronic continuum, (ii) a broad scattering response near 600 cm^{-1} associated with electronic scattering that has developed due to the formation of a charge gap, and (iii) a two-magnon (2M) excitation near 100 cm^{-1} associated with spin-pair excitations of the Ru ions. In the following, we consider in greater detail the temperature and x dependence of each of these excitations.

Unlike Sr_2RuO_4 , which has the ideal tetragonal K_2NiF_4 structure, Ca-substitution significantly distorts the crystal structure of CSRO, causing both a rotation of the RuO_6 -octahedra around the c -axis, and a tilt of the octahedra around an axis lying in the RuO_2 planes. As a result, Ca_2RuO_4 is orthorhombic (Pbca-D_{2h}^{15}),⁷ and a factor group analysis indicates that there should be 9 B_{1g} symmetry Raman-active optical phonons¹² involving Ca/Sr, apical oxygen, and in-plane oxygen ions. One notes from Fig. 1 that while the optical phonon spectrum of Ca_2RuO_4 exhibits narrow and symmetric phonon lineshapes at 10 K , with increasing Sr substitution there is a significant broadening of the linewidths — and the appearance of

a distinct “asymmetric” Fano profile — associated with many of the phonons. This is indicative of an increase in electron-phonon coupling with increasing Sr substitution.¹³ The phonon linewidth and asymmetric parameters can be obtained from fits to a Fano profile, $I(\omega)=I_0(q+\epsilon)^2/(1+\epsilon^2)$, where $\epsilon = (\omega-\omega_0)/\Gamma$, ω_0 is the phonon frequency, Γ is the effective phonon linewidth, and q is the asymmetry parameter that is related to the electron-phonon coupling strength V and the imaginary part of the electronic susceptibility ρ according to $1/q \sim V\rho$.^{13,14} Indeed, as shown in the inset of Fig. 1, Sr substitution results in a significant increase in the electron-phonon coupling and phonon linewidth associated with the 456 cm^{-1} B_{1g} mode.

The MI transition in CSRO is driven by an elongation of the RuO_6 octahedron in the metal phase.⁷ Figure 2 illustrates that striking changes in the B_{1g} Raman scattering response of CSRO for $x = 0.09$ are observed through T_{MI} (~ 220 K) upon heating. For example, a number of phonon modes disappear rapidly above T_{MI} , providing a clear demonstration that the MI transition is accompanied by a structural change from the S-Pbca phase to the less distorted L-Pbca phase.⁷ Additionally, as temperature is increased toward T_{MI} , the phonons soften and broaden significantly, reflecting elongation of the RuO_6 octahedra along the c -axis and increased interaction with thermally-excited carriers, respectively. These changes are summarized in Fig. 2 (b) for the 456 cm^{-1} B_{1g} mode, which we tentatively attribute to the apical oxygen vibration, based upon both the high frequency of this mode and a comparison with similar modes in cuprates and other ruthenates.¹⁵ The phonon frequency and linewidth parameters were obtained at different temperatures from fits to a Fano profile. Note that the phonon linewidth is enhanced as the temperature approaches T_{MI} , indicating a mixed phase regime and/or enhanced damping of the phonon response due to increased structural instability near the MI transition. Above T_{MI} , most of the B_{1g} phonons observed below T_{MI} are absent, and the two remaining optical phonons show no further phonon frequency and linewidth changes at least up to the room temperature, suggesting that in the metal phase, the crystal structure is stabilized in the L-Pbca configuration.

That the MI transition is first-order is apparent by comparing the Raman spectra of CSRO ($x = 0.09$) obtained during thermal cycle. The inset of Fig. 2 (a) illustrates that the 175 K spectrum obtained upon cooling exhibits the simple phonon spectrum indicative of the metallic phase, while the 175 K spectrum obtained upon heating exhibits the complex phonon spectra associated with the insulating phase. This is consistent with evidence for

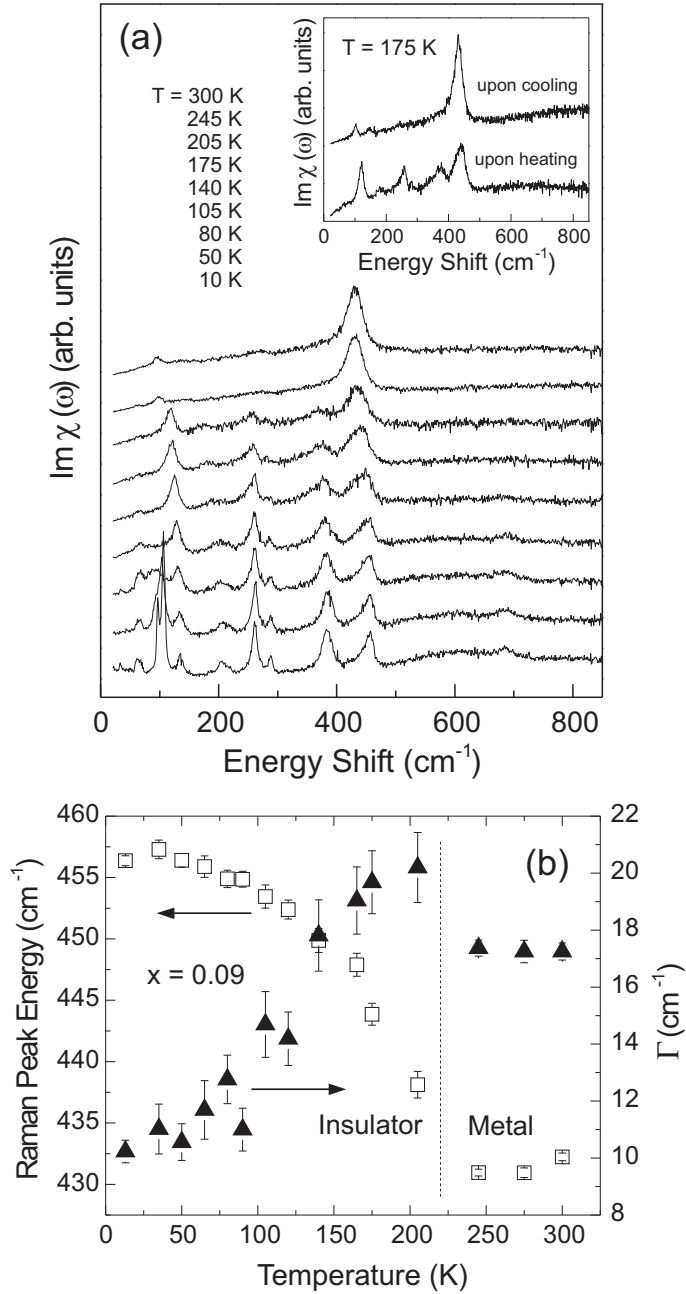


FIG. 2: (a) Temperature-evolution of the Raman scattering spectra through T_{MI} for the $x = 0.09$ sample upon heating. The inset shows 175 K Raman scattering spectra obtained by alternately cooling and heating the $x = 0.09$ sample, showing structural hysteresis. Each spectrum is shifted vertically for clarity. (b) Temperature-evolution of the 456 cm^{-1} Raman peak energies (open squares) and linewidths (filled triangles).

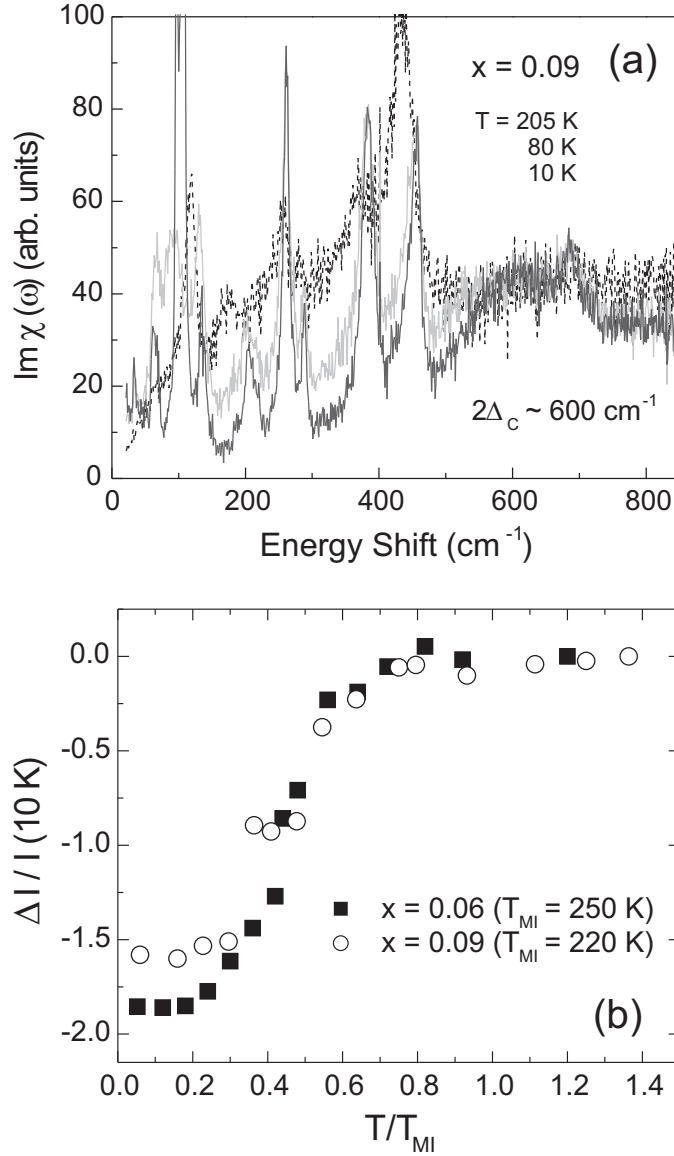


FIG. 3: (a) Electronic Raman scattering spectra from the $x = 0.09$ sample upon heating, showing a charge gap closing through the MI transition. (b) Fractional changes of the charge gap responses as a function of the reduced temperature for $x = 0.06$ (filled squares) and 0.09 (open circles).

hysteresis observed in CSRO ($0 \leq x < 0.2$) by transport and neutron diffraction,^{7,8} based upon which $T_{MI} = 155$ K upon cooling and 220 K upon heating have been estimated in CSRO for $x = 0.09$.

Evidence for the first-order nature of the phase transition is also indicated in the evolution of a charge gap in the electronic continuum below T_{MI} . This is illustrated, for example, in the temperature-dependent Raman spectra of CSRO for $x = 0.09$ shown in Fig. 3 (a),

in which one observes below T_{MI} a suppression of electronic scattering strength below $\sim 600 \text{ cm}^{-1}$, and a redistribution of this scattering strength to a broad scattering response between 550 and 650 cm^{-1} . With increasing temperature toward T_{MI} , the charge gap closes systematically. This behavior is indicative of the opening of a charge gap in CSRO, and is similar to that observed below the MI transitions of other correlation gap insulators such as FeSi,¹⁶ SmB₆,¹⁷ and Ca₃Ru₂O₇,¹⁸ and described theoretically.¹⁹ To examine the development of the charge gap more quantitatively, we plot in Fig. 3 (b) the temperature-dependence of the fractional change in the integrated electronic scattering response, $\Delta I/I(10 \text{ K})$, for $x = 0.09$ and 0.06 , where $\Delta I = I(T) - I(300 \text{ K})$ and $I(T) = \int_0^{2\Delta_c} \text{Im}\chi(\omega) d\omega$ is the integrated spectral weight of the electronic Raman scattering response below $2\Delta_c = 600 \text{ cm}^{-1}$. The overall temperature-dependence of the fractional intensity shown in Fig. 3 (b) is similar to those observed in FeSi, SmB₆, and Ca₃Ru₂O₇. There is one notable difference, however, in that the charge gap in CSRO closes with increasing temperature well below the MI transition temperature. We attribute this behavior to the likely coexistence of insulating (S-Pbca) and metallic (L-Pbca) phase regions. In particular, in the temperature range between $155 \text{ K} - 220 \text{ K}$, CSRO at $x = 0.09$ is primarily in the metal phase upon cooling, but is primarily in the insulating phase upon heating. Consequently, during the thermal cycle, some metal components are known to coexist with insulating components in this temperature range. Indeed, neutron scattering⁷, resistivity and susceptibility⁸ measurements of CSRO for $x < 0.2$ clearly indicate thermal hysteresis through the MI transition; further, neutron scattering measurements clearly reveal the coexistence of S-Pbca and L-Pbca phases⁷ in this temperature range.

Finally, for $T < T_N$ in CSRO at $x = 0, 0.06$, and 0.09 , a peak in the Raman scattering response is observed to develop rapidly near 100 cm^{-1} in the B_{1g} scattering geometry (see Figs. 1 and 4 (a)). This response is associated with 2M scattering, involving a photon-induced flipping of neighboring spins on nearest-neighbor Ru-4d⁴ sites; this scattering response not only reveals the presence of AF correlations in the ground state of this system, but provides useful information on the superexchange coupling constant J .^{18,20,21,22,23} Figure 4 summarizes the temperature-dependent energy renormalization, linewidths, and intensity change of the 2M scattering response of CSRO. With increasing temperature, the 2M scattering response diminishes in intensity, shifts to lower energies, and broadens, similar to the behavior observed in the bilayer ruthenate system Ca₃Ru₂O₇.¹⁸ Using the fact that the 2M peak energy

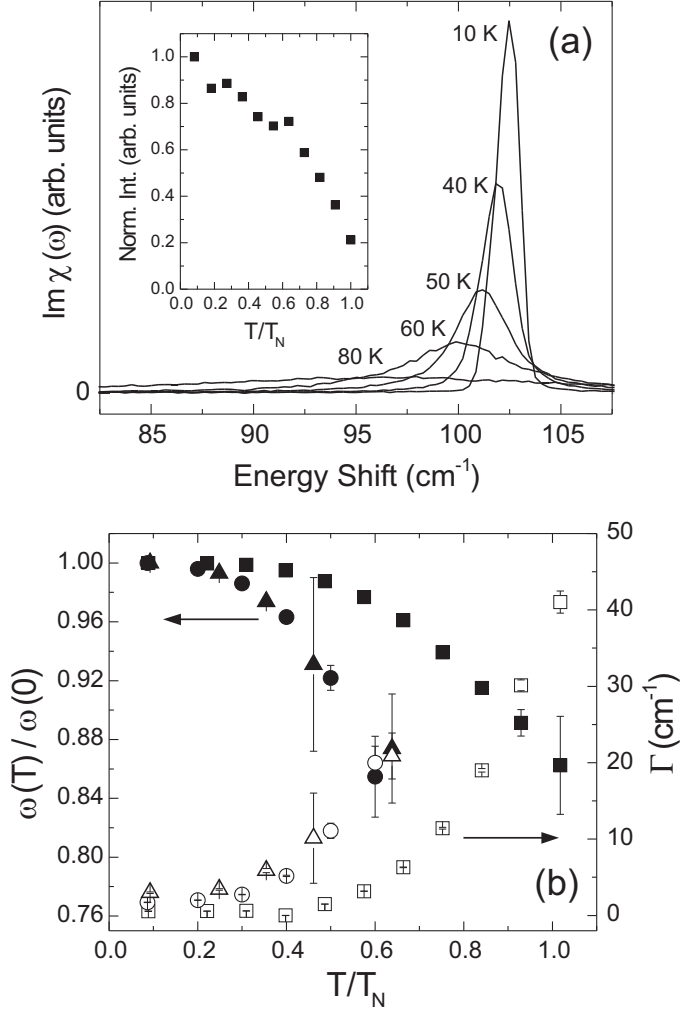


FIG. 4: (a) The 2M scattering response of Ca_2RuO_4 at the elevated temperature. The inset shows the spectrally integrated intensity change of the 2M responses as a function of the normalized temperature. (b) Summary of the normalized 2M peak energy changes for $x = 0$ (filled squares), 0.06 (filled circles), and 0.09 (filled triangles), respectively, and the corresponding spectral width changes for $x = 0$ (open squares), 0.06 (open circles), and 0.09 (open triangles), respectively, as a function of the normalized temperature.

for $S = 1$ AF insulators is given by $6.7 J$,²² the estimated in-plane exchange energies between nearest-neighbor Ru- $4d^4$ sites are 15.22, 15.37, and 15.97 cm^{-1} for the $x = 0$, 0.06, and 0.09 samples, respectively. Interestingly, in spite of a significant change in the Néel temperature with Sr substitution ($T_N = 113$ K, 150 K, 141 K for $x = 0$, 0.06, and 0.09, respectively), the 2M energy is relatively insensitive to Sr substitution, indicating that the local AF exchange

coupling is relatively unaffected by Sr substitution at these values of x . This is consistent with recent pressure-dependent Raman studies of Ca_2RuO_4 , which show that the 2M energies are relatively insensitive to pressure up to the pressure-induced MI transition.²⁴ Both of these results support the conclusion that antiferromagnetism is suppressed with increasing Sr substitution and pressure, not by affecting the AF exchange coupling, but rather by reducing the volume-fraction of distorted S-Pbca phase regions that support orbital polarization and AF order.²⁴ Figure 4 (b) also shows that the 2M scattering responses in the $x = 0, 0.06,$ and 0.09 samples exhibit substantially different temperature-dependences. In particular, in comparison to the $x = 0$ sample, Sr substitution causes a much more dramatic renormalization of the 2M energy and linewidth with increasing temperature. This observation suggests that the Sr substitution causes a substantially larger suppression of magnetic correlations with increasing temperature than in the $x = 0$ material. This is presumably due either to the disorder introduced in the magnetic lattice when Sr is introduced, and/or to the increased electronic contribution introduced with Sr substitution, which increases the amount of magnon energy and lifetime renormalization compared to the $x = 0$ material.²³

In conclusion, Raman scattering results on CSRO for $0 \leq x < 0.2$ provide substantial insight into the interplay among the spin, charge, and lattice dynamics through the MI and magnetic phase changes. In particular, this study demonstrates that the Sr substitution for Ca significantly affects the magnetic and electronic excitations, as evidenced by a substantial increase in the renormalization of the 2M energies and linewidths, and by an increase of the electron-phonon interactions. The temperature-dependent evolution of the Raman scattering response shows that the MI transition is accompanied by both a significant change in the phonon spectrum and the development of a charge gap. Both the hysteretic behavior of the phonon temperature-dependence, as well as the temperature-dependent evolution of the charge gap, are indicative of a phase coexistence regime involving L-Pbca and S-Pbca components near T_{MI} .

This work was supported by the Department of Energy through grant DEFG02-96ER45439, and by the National Science Foundation through grant NSF DMR-0244502. H.R. acknowledges a support of this work in part by the research fund of Chonbuk National

University.

- ¹ Y. Maeno *et al.*, Nature (London) **372**, 532 (1994).
- ² V. I. Anisimov *et al.*, Eur. Phys. J. B **25**, 191 (2002).
- ³ T. Hotta and E. Dagotto, Phys. Rev. Lett. **88**, 17201 (2002).
- ⁴ J. S. Lee *et al.*, Phys. Rev. Lett. **89**, 257402 (2002).
- ⁵ S. Nakatsuji and Y. Maeno, Phys. Rev. Lett. **84**, 2666 (2000); S. Nakatsuji and Y. Maeno, Phys. Rev. B **62**, 6458 (2000).
- ⁶ S. Nakatsuji, S. Ikeda, and Y. Maeno, J. Phys. Soc. Jpn. **66**, 1868 (1997).
- ⁷ M. Braden *et al.*, Phys. Rev. B **58**, 847 (1998); O. Friedt *et al.*, Phys. Rev. B **63**, 174432 (2001).
- ⁸ S. Nakatsuji *et al.*, unpublished.
- ⁹ H. Fukazawa, S. Nakatsuji, and Y. Maeno, Physica B **281&282**, 613 (2000).
- ¹⁰ C. S. Alexander *et al.*, Phys. Rev. B **60**, R8422 (1999).
- ¹¹ S. Nakatsuji and Y. Maeno, J. Solid State Chem. **156**, 26 (2001).
- ¹² High-resolution spectra reveal that the unresolved B_{1g} phonon response at ~ 267 cm^{-1} from the Ca_2RuO_4 sample consists of two B_{1g} phonons.
- ¹³ U. Fano, Phys. Rev. **124**, 1866 (1961).
- ¹⁴ S. Naler *et al.*, Phys. Rev. B **65**, 92401 (2002).
- ¹⁵ S. Sakita *et al.*, Phys. Rev. B **63**, 134520 (2001); R. Liu *et al.*, Phys. Rev. B **45**, 7392 (1992).
- ¹⁶ P. Nyhus, S. L. Cooper, and Z. Fisk, Phys. Rev. B **51**, 15626 (1995).
- ¹⁷ P. Nyhus *et al.*, Phys. Rev. B **52**, R14308 (1995); P. Nyhus *et al.*, Phys. Rev. B **55**, 12488 (1997).
- ¹⁸ H. L. Liu *et al.*, Phys. Rev. B **60**, R6980 (1999).
- ¹⁹ J. K. Freericks, T. P. Devereaux, and R. Bulla, Phys. Rev. B **64**, 233114 (2001).
- ²⁰ P. A. Fleury and R. Loudon, Phys. Rev. **166**, 514 (1968).
- ²¹ K. B. Lyons *et al.*, Phys. Rev. B **37**, 2353 (1988).
- ²² S. Sugai *et al.*, Phys. Rev. B **42**, 1045 (1990).
- ²³ W. H. Weber and G. W. Ford, Phys. Rev. B **40**, 6890 (1989).
- ²⁴ C. S. Snow *et al.*, Phys. Rev. Lett. **89**, 226401 (2002).